Some advances in the lattice Boltzmann method for flows in the presence of curved boundaries and non-uniform magnetic fields

by

H.S. Tavares[1], B. Magacho[1], L. Moriconi[1], J.B. Loureiro[2]

[1] Instituto de Física, Universidade Federal do Rio de Janeiro (UFRJ)

[2] Programa de Engenharia Mecânica, Universidade Federal do Rio de Janeiro (UFRJ)

Outline

- Chapman-Enskog: From Boltzmann to Navier-Stokes equations
- Traditional lattice Boltzmann method
- Simplified LBM for momentum and continuity equations
- Extension for advection-diffusion equations (ADE)
- Magnetohydrodynamic flows (MHD)
- Simplified LBM for MHD equations
- Some numerical results
- Central-moments-based LBM for MHD flows
- Conclusions

The Boltzmann equation is an integro-differential equation for the probability density function $f(\mathbf{x}, \mathbf{v}, t)$ in six-dimensional space of a particle position $\mathbf{x} \in \mathbb{R}^3$ and momentum $\mathbf{v} \in \mathbb{R}^3$ given by

$$\partial_t f + \nabla_{\mathbf{x}} f \cdot \mathbf{v} + \frac{\mathbf{F}}{\rho} \cdot \nabla_{\mathbf{v}} f = Q(f, f), \tag{1}$$

where $Q(f, f)$ is collision integral, $\mathbf{F}$ is the body force, ρ is macroscopic mass density of the system, and $\nabla_{\mathbf{x}}$ and $\nabla_{\mathbf{v}}$ are gradients with respect to the position $\mathbf{x}$ and velocity $\mathbf{v}$ coordinates, respectively.

It can be shown that the collision integral $Q(f, f)$ has at least five invariants, i.e., a set of functions $\xi_k, \ k = 1, 2, 3, 4, 5$, satisfying

$$\int \xi_k(\mathbf{v}) Q(f, f) d\mathbf{v} = 0, \tag{2}$$

which are $\xi_1 = 1$, $(\xi_2, \xi_3, \xi_4) = \mathbf{v}$ and $\xi_5 = |\mathbf{v}|^2$, with the integration being performed in $\mathbb{R}^3$

It can be shown that the collision integral $Q(f,f)$ has at least five invariants, i.e., a set of functions $\xi_k, \; k = 1,2,3,4,5$, satisfying

$$\int \xi_k(\mathbf{v}) Q(f,f) d\mathbf{v} = 0, \tag{3}$$

which are $\xi_1 = 1$, $(\xi_2, \xi_3, \xi_4) = \mathbf{v}$ and $\xi_5 = |\mathbf{v}|^2$, with the integration being performed in $\mathbb{R}^3$.

A general collision invariant can be written as linear combinations of the functions ξ_k. The invariants are associated to some important macroscopic quantities in the system

$$\text{mass density:} \quad \int f d\mathbf{v} = \rho, \tag{4}$$

$$\text{momentum:} \quad \int f \mathbf{v} d\mathbf{v} = \rho \mathbf{u}, \tag{5}$$

$$\text{energy:} \quad \frac{1}{2} \int f |\mathbf{v}|^2 d\mathbf{v} = \rho E. \tag{6}$$

A set of **conservation laws** for each of this quantities can be obtained multiplying the Boltzmann equation (1) by a **collision invariant** and subsequently integrating with respect to the velocity. For example, for $\xi_k = 1$, we have

$$\frac{\partial}{\partial t}\left(\int f d\mathbf{v}\right) + \nabla_{\mathbf{x}} \cdot \left(\int f \mathbf{v} d\mathbf{v}\right) + \frac{\mathbf{F}}{\rho} \cdot \left(\int \nabla_{\mathbf{v}} f d\mathbf{v}\right) = \int Q(f,f) d\mathbf{v} = 0 \quad \Rightarrow \quad (7)$$

$$\Rightarrow \quad \partial_t \rho + \nabla \cdot (\rho \mathbf{u}) = 0, \quad (8)$$

obtaining to the **continuity equation**. Similarly, if we take first moment of the Boltzmann equation we find

$$\frac{\partial(\rho \mathbf{u})}{\partial t} + \nabla \cdot \Pi = \mathbf{F}, \quad (9)$$

where Π is the **momentum flux tensor** given by

$$\Pi = \int f \mathbf{v} \otimes \mathbf{v} d\mathbf{v}. \quad (10)$$

By splitting the particle velocity $\mathbf{v} = \mathbf{u} + \mathbf{w}$, where $\mathbf{w}$ is the relative velocity, we obtain

$$\Pi = \rho \mathbf{u} \otimes \mathbf{u} + \int f \mathbf{w} \otimes \mathbf{w} d\mathbf{v}. \tag{11}$$

Thus, the equation (9) becomes the *Cauchy momentum equation*

$$\frac{\partial(\rho \mathbf{u})}{\partial t} + \nabla \cdot (\rho \mathbf{u} \otimes \mathbf{u}) = \nabla \cdot \mathbf{P} + \mathbf{F}. \tag{12}$$

However, in this equation we do not know explicitly the *stress tensor*

$$\mathbf{P} = -\int (\mathbf{w} \otimes \mathbf{w}) f d\mathbf{v}. \tag{13}$$

We can approximate this stress tensor using an explicit approximation for the distribution function f.

Boltzmann showed in 1872 that the entropy function,

$$H(t) = \int f(\mathbf{x}, \mathbf{v}, t) \ln(f(\mathbf{x}, \mathbf{v}, t)) d\mathbf{x} d\mathbf{v}, \tag{14}$$

where f is any function satisfying the Boltzmann equation, fulfills the equation

$$\frac{dH}{dt} \leq 0. \tag{15}$$

The equality in (15) holds for a distribution f^{eq} given by

$$f^{eq}(\rho, \mathbf{u}, \mathbf{v}, T) = \rho \left(\frac{1}{2\pi RT} \right)^{3/2} e^{-|\mathbf{v}-\mathbf{u}|^2/(2RT)}, \tag{16}$$

where T is the temperature and R is the ideal gas constant. This is the so-called the **local equilibrium distribution** of the system. A direct calculation also shows that $Q(f^{eq}, f^{eq}) = 0$.

The collision operators commonly used in numerical methods for the Boltzmann equation are based on the **Bhatnagar-Gross-Krook (BGK)** collision operator:

$$\Omega(f,f) = -\frac{1}{\tau}(f - f^{eq}), \tag{17}$$

where τ is known as the **relaxation time**, which determines the speed of the convergence to the equilibrium state of the system.

If we approximate $f \simeq f^{eq}$, the equation (12) becomes the **Euler momentum equation**

$$\frac{\partial(\rho\mathbf{u})}{\partial t} + \nabla\cdot(\rho(\mathbf{u}\otimes\mathbf{u})) = \nabla p + \mathbf{F}, \tag{18}$$

where p is the pressure given by

$$p = \frac{1}{3}\int |\mathbf{w}|^2 f^{eq}(\mathbf{x},\mathbf{v},t)d\mathbf{v}. \tag{19}$$

A more general approximation for f, which accounts the non-equilibrium effects, is obtained using the **Chapman-Enskog analysis**. It consists in the expansion of f as a perturbation around f^{eq} given by

$$f = f^{eq} + \sum_{k=1}^{\infty} \varepsilon^k f^{(k)}, \tag{20}$$

where ε labels each term's order and is often stated in the literature as proportional to the **Knudsen number** $\mathrm{Kn} = \ell_{mfp}/L$ of the system, defined as the ratio between the mean free path ℓ_{mfp} and the representative physical length scale L.

Analogously, the operators ∂_t and $\nabla_{\mathbf{x}}$ have to be defined such that they are consistent with the conservation laws.

To the first order approximation $f \approx f^{eq} + \varepsilon f^{(1)}$, we obtain the Navier-Stokes equations with the following stress tensor

$$\mathbf{P} \simeq -p\mathbf{I} + \frac{\eta}{2}(\nabla\mathbf{u} + \nabla\mathbf{u}^T), \tag{21}$$

from the equation (13), where η is the dynamic viscosity. Thus, from a **solution of the Boltzmann equation** for a given system we can derive a **solution for the Navier-Stokes equations** for the same case.

In the **lattice Boltzmann method** (LBM) the basic quantity is the **discrete-velocity distribution function** $f_i(x, t)$, often called the **particle populations**, it represents the density of particles with velocity $\mathbf{c}_i$ at position $\mathbf{x}$ and time t.

By discretizing the Boltzmann equation in velocity space, physical space, and time, we obtain the **discrete Boltzmann equation**

$$f_i(\mathbf{x} + \mathbf{c}_i \Delta t, t + \Delta t) = f_i(\mathbf{x}, t) + \Omega_i(\mathbf{x}, t). \tag{22}$$

This equation expresses that a particle $f_i(\mathbf{x}, t)$ moves with velocity $\mathbf{c}_i$ to the nearest neighbors after a time step Δt.

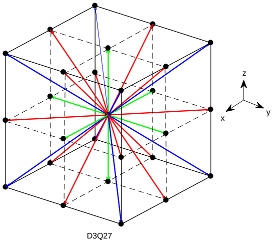

Figure: Lattice velocities for D3Q27 scheme.

Analogously, the mass density and momentum $\rho\mathbf{u}$ at (x, t) can be found through weighted sums known as moments of f_i as

$$\rho(\mathbf{x}, t) = \sum_i f_i(\mathbf{x}, t), \tag{23}$$

$$\rho\mathbf{u}(\mathbf{x}, t) = \sum_i \mathbf{c}_i f_i(\mathbf{x}, t). \tag{24}$$

The main difference between f_i and the **continuous distribution** function f is that all of the argument variables of f_i are **discrete**, with the subscript i referring to a finite discrete set of velocities $\mathbf{c}_i$.

The discrete version of the BGK-collision operator is given by Ω_i defined as

$$\Omega_i(f,f) = -\frac{f_i - f_i^{eq}}{\tau}. \tag{25}$$

The equilibrium distribution is calculated by maximizing the entropy

$$S(\rho,\mathbf{u}) = -\sum_i f^{eq}(\rho,\mathbf{u}) \ln\left(\frac{f^{eq}(\rho,\mathbf{u})}{w_i}\right), \tag{26}$$

for given constraints, which for case under consideration are the mass and momentum densities given by (23) and (24), i.e.,

$$\sum_i f_i^{eq} = \sum_i f_i = \rho, \tag{27}$$

$$\sum_i \mathbf{c}_i f_i^{eq} = \sum_i \mathbf{c}_i f_i = \rho\mathbf{u}. \tag{28}$$

We obtain as a minimum of S the following distribution:

$$f_i^{eq}(\rho, \mathbf{u}) = \rho w_i \left(1 + \frac{\mathbf{c}_i \cdot \mathbf{u}}{c_s^2} + \frac{(\mathbf{c}_i \cdot \mathbf{u})^2}{2c_s^4} - \frac{\mathbf{u} \cdot \mathbf{u}}{2c_s^2}\right), \tag{29}$$

where the weights w_i are associated to the velocity set D2Q9.

Using the BGK approximation in the discrete Boltzmann equation, we obtain the lattice BGK equation:

$$f_i(\mathbf{x} + \mathbf{c}_i, t+1) = f_i(\mathbf{x}, t) - \frac{1}{\tau}\left(f_i(\mathbf{x}, t) - f_i^{eq}(\rho, \mathbf{u})\right). \tag{30}$$

The simplest way to initialize the populations at the initial time $t = 0$ is to set

$$f_i(\mathbf{x}, t=0) = f_i^{eq}(\rho(\mathbf{x}, t=0), \mathbf{u}(\mathbf{x}, t=0)). \tag{31}$$

Using Chapman-Enskog expansion the kinematic shear viscosity is associated to the relaxation time by the equation

$$\nu = c_s^2 \left(\tau - \frac{1}{2} \right) \delta t, \tag{32}$$

where $c_s = c/\sqrt{3}$ is the speed of sound in l.b.u.. In addition, the momentum flux tensor $\mathbf{P}$ is approximated from f_i as

$$\mathbf{P} \simeq \left(1 - \frac{1}{2\tau} \right) \sum_i (\mathbf{c}_i \otimes \mathbf{c}_i) f_i \tag{33}$$

analogously to the formula (13) in the continuum case. The **viscous contribution** σ to the momentum flux tensor is approximated as

$$\sigma \simeq \left(1 - \frac{\delta t}{2\tau} \right) \sum_i (\mathbf{c}_i \otimes \mathbf{c}_i)(f_i - f_i^{eq}) = \rho\nu(\nabla\mathbf{u} + \nabla\mathbf{u}^T). \tag{34}$$

where ν is the kinematic viscosity.

As a consequence of the Chapman-Enskog multiscale analysis, we obtain the following final equations

$$\sum_{i=1}^{N} \left[\frac{\partial f_i^{eq}}{\partial t} + \mathbf{c}_i \cdot \nabla f_i^{eq} \right] = 0, \tag{35}$$

$$\sum_{i=1}^{N} \mathbf{c}_i \left[\frac{\partial f_i^{eq}}{\partial t} + \mathbf{c}_i \cdot \nabla f_i^{eq} + \left(1 - \frac{1}{2\tau}\right) D f_i^{(1)} \right] = 0, \tag{36}$$

with

$$\sum_{i=1}^{N} f_i^{(1)} = 0 \tag{37}$$

$$\sum_{i=1}^{N} \mathbf{c}_i f_i^{(1)} = 0. \tag{38}$$

The non-equilibrium term can be approximated as

$$f^{(1)}(\mathbf{r}, t) \simeq -\tau \left[f^{eq}(r, t) - f^{eq}(r - \mathbf{c}_i \delta t, t - \delta t) \right]. \tag{39}$$

From the first order of the Chapman-Enskog expansion

$$\sum_{i=0}^{N}\left[\frac{\partial f_i^{eq}}{\partial t}+\mathbf{c}_i\cdot\nabla f_i^{eq}\right]=0, \tag{40}$$

We approximate the RHS of the equation (40) by a forward finite difference schemes

$$\frac{\partial f_i^{eq}}{\partial t}=\frac{f_i^{eq}(\mathbf{x},t+\delta t)-f_i^{eq}(\mathbf{x},t)}{\delta t}, \tag{41}$$

The second term of the LHS of the equation (40) is discretized using the the following finite difference scheme

$$\mathbf{c}_i\cdot\nabla f_i^{eq}=-\frac{f_i^{eq}(\mathbf{x}+\mathbf{c}_i\delta t,t)-4f_i^{eq}(\mathbf{x},t)+3f_i^{eq}(\mathbf{x}-\mathbf{c}_i\delta t,t)}{2\delta x} \tag{42}$$

By replacing the expressions derived in Equations (41) and (42) in Equation (40), one obtains

$$\sum_{i=1}^{N}\frac{f_i^{eq}(\mathbf{x},t+\delta t)-f_i^{eq}(\mathbf{x},t)}{\delta t}+\frac{f_i^{eq}(\mathbf{x},t)-f_i^{eq}(\mathbf{x}-c_i\delta t,t)}{\delta x}=0. \tag{43}$$

The equation (43) can be rewrite as:[1].

$$\rho(\mathbf{x}, t+\delta t) = \frac{3}{2}\sum_{i=1}^{N} f^{eq}(\mathbf{x}-\mathbf{c}_i\delta t, t) - \sum_{i=1}^{N} f_i^{eq}(\mathbf{x}, t) + \frac{1}{2}\sum_{i=1}^{N} f_i^{eq}(\mathbf{x}+\mathbf{c}_i\delta t, t) \tag{44}$$

[1] Delgado-Gutiérrez, Arturo, et al. International Journal for Numerical Methods in Fluids 93.7 (2021): 2339-2361.

The derivation for the momentum equation follows a similar treatment compared to the derivation for the density.

$$\sum_{i=1}^{N} \mathbf{c}_i \left[\frac{\partial f_i^{eq}}{\partial t} + \mathbf{c}_i \cdot \nabla f_i^{eq} + \left(1 - \frac{1}{2\tau}\right) D f_i^{(1)} \right] = 0 \tag{45}$$

By explicitly expressing $Df_i^{(1)}$ as

$$Df_i^{(1)} = \frac{\partial f_i^{(1)}}{\partial t_0} + \mathbf{c}_i \cdot \nabla f_i^{(1)}, \tag{46}$$

applying the directional approach for the gradient operation

$$\sum_{i=1}^{N} \mathbf{c}_i D f_i^{(1)} = \sum_{i=1}^{N} \mathbf{c}_i \frac{\partial f^{(1)}}{\partial c}. \tag{47}$$

The term $\frac{\partial f_i^{(1)}}{\partial t}$ can be expressed as

$$\frac{\partial f_i^{(1)}}{\partial t} = \frac{-\tau[f_i^{eq}(\mathbf{x} + \mathbf{c}_i \delta t, t) - f_i^{eq}(\mathbf{x}, t) + f_i^{eq}(\mathbf{x} - \mathbf{c}_i \delta t, t)]}{\delta x}. \tag{48}$$

The second term from Equation (45) can be also simplified by using a second order central difference:

$$\mathbf{c}_i \cdot \nabla f_i^{eq} = \frac{f_i^{eq}(\mathbf{x}+\mathbf{c}_i\delta t, t) - f_i^{eq}(\mathbf{x}-\mathbf{c}_i\delta t, t)}{2\delta x}. \tag{49}$$

Combining all the finite differences proposed, we obtain the following expression for the computation of the macroscopic momentum:[2].

$$\begin{aligned} \mathbf{m}(\mathbf{x}, t+\delta t) &= \sum_{i=1}^{N} \mathbf{c}_i f_i^{eq}(\mathbf{x}-\mathbf{c}_i\delta t, t) + \\ &+ (\tau-1)[f_i^{eq}(\mathbf{x}+\mathbf{c}_i\delta t, t) - 2f_i^{eq}(\mathbf{x}, t) + f_i^{eq}(\mathbf{x}-\mathbf{c}_i\delta t, t)]. \end{aligned} \tag{50}$$

where $\mathbf{m}(\mathbf{x}, t+\delta t) = \rho(\mathbf{x}, t+\delta t)\mathbf{u}(\mathbf{x}, t+\delta t)$.

[2] Delgado-Gutiérrez, Arturo, et al. International Journal for Numerical Methods in Fluids 93.7 (2021): 2339-2361.

Now consider a general the advection- diffusion equation (ADE) for a scalar field c:

$$\frac{\partial c}{\partial t} + \nabla \cdot (c\mathbf{u}) = \nabla \cdot (D\nabla c) + q \tag{51}$$

The left-hand side describes the advection of C in the presence of an external fluid velocity u, while the right-hand side contains a diffusion term with diffusion coefficient D and a possible source term q.

The ADE and the Navier-Stokes equation have similarities. It is possible adapt the lattice Boltzmann method in order to solve general advection-diffusion equations.

It turns out that the LBE

$$g_i(\mathbf{x} + \mathbf{c}_i \delta t, t + \delta t) = g_i(\mathbf{x}, t) - \frac{1}{\tau_c}(g_i(\mathbf{x}, t) - g_i^{eq}(\mathbf{x}, t)) + Q_i, \tag{52}$$

and suitable source terms Q_i solves the ADE for the **concentration field** $c = \sum_{i=1}^{N} g_i$. This collision operator results in a diffusion coefficient

$$D = c_s^2 \left(\tau_g - \frac{1}{2} \right) \delta t. \tag{53}$$

where τ_c is the respective relaxation time.

The **equilibrium distribution** typically assumes the form

$$g_i^{eq}(c, \mathbf{u}) = w_i c \left(1 + \frac{\mathbf{c}_i \cdot \mathbf{u}}{c_s^2} + \frac{(\mathbf{c}_i \cdot \mathbf{u})^2}{2c_s^4} - \frac{\mathbf{u} \cdot \mathbf{u}}{2c_s^2} \right). \tag{54}$$

The lattice Boltzmann equation (LBE) can be written as

$$g_i(\mathbf{x} + \mathbf{c}_i \delta t, t) - g_i(\mathbf{x}, t) = \frac{g_i^{eq}(\mathbf{x}, t) - g_i(\mathbf{x}, t)}{\tau_c}, \quad (55)$$

If we apply a Taylor series expansion at the left-hand side of (55) followed by a **Chapman–Enskog multiscale analysis**, it is possible to write the following equations

$$\sum_i \left[\frac{\partial g_i^{eq}}{\partial t} + \mathbf{c}_i \cdot \nabla g_i^{eq} + \left(1 - \frac{1}{2\tau_c}\right) D_i g_i^{(1)} \right] = 0. \quad (56)$$

where

$$\sum_i g_i^{(1)} = 0 \quad (57)$$

$$\sum_i \mathbf{c}_i g_i^{(1)} = 0. \quad (58)$$

It is possible to write[3].

$$\begin{aligned}
\frac{\partial g_{ix}^{eq}}{\partial t_0} &= g_{ix}^{eq}(\mathbf{x}, t+\delta t) - g_{ix}^{eq}(\mathbf{x}, t) \\
\mathbf{c}_i \cdot \nabla g_{ix}^{eq} &= \frac{g_{ix}^{eq}(\mathbf{x}+\mathbf{c}_i\delta t, t) - g_{ix}^{eq}(\mathbf{x}-\mathbf{c}_i\delta t, t)}{2\delta x} \\
\sum_i D_i g_{ix}^{(1)} &= \sum_i \frac{\partial g_{ix}^{(1)}}{\partial c_i} \simeq \sum_i \frac{g_{ix}^{(1)}(\mathbf{x}+\mathbf{c}_i\delta t, t) - g_{ix}^{(1)}(\mathbf{x}, t)}{\delta x} = \\
&= \sum_i -\tau_c \left[g_{ix}^{eq}(\mathbf{x}+\mathbf{c}_i\delta t, t) - 2g_{ix}^{eq}(\mathbf{x}, t) + g_{ix}^{eq}(\mathbf{x}-\mathbf{c}_i\delta t, t)\right].
\end{aligned}$$

Then, we get

$$\sum_i \Big[g_{ix}^{(0)}(\mathbf{x}, t+\delta t) + 2(\tau_c - 1)g_{ix}^{(0)}(\mathbf{x}, t) - \\ -(\tau_c - 1)g_{ix}^{(0)}(\mathbf{x}+\mathbf{c}_i\delta t, t) - \tau_g g_{ix}^{(0)}(\mathbf{x}-\mathbf{c}_i\delta t, t) = 0\Big]. \qquad (59)$$

[3] De Rosis, Alessandro, Ruizhi Liu, and Alistair Revell. Physics of Fluids 33.8 (2021): 085114.

By noticing that

$$\sum_i g_i^{eq}(\mathbf{x}, t + \delta t) = c(\mathbf{x}, t + \delta t), \tag{60}$$

$$\sum_i g_i^{eq}(\mathbf{x}, t) = c(\mathbf{x}, t), \tag{61}$$

we end up with

$$\begin{aligned} c(\mathbf{x}, t + \Delta t) &= \sum_{i=1}^{N} g_i^{eq}(\mathbf{x} - \mathbf{c}_i \delta t, t) + \\ &+ (\tau_c - 1)[g_i^{eq}(\mathbf{x} + \mathbf{c}_i \delta t, t) - 2 g_i^{eq}(\mathbf{x}, t) + g_i^{eq}(\mathbf{x} - \mathbf{c}_i \delta t, t)]. \end{aligned} \tag{62}$$

Considering the following expression for the equilibrium distributions:

$$f_i^{eq}(\rho, \mathbf{u}) = w_i \rho \left(1 + \frac{\mathbf{c}_i \cdot \mathbf{u}}{c_s^2} + \frac{(\mathbf{c}_i \cdot \mathbf{u})^2}{2c_s^4} - \frac{\mathbf{u} \cdot \mathbf{u}}{2c_s^2}\right), \quad (63)$$

$$g_i^{eq}(c, \mathbf{u}) = w_i c \left(1 + \frac{\mathbf{c}_i \cdot \mathbf{u}}{c_s^2} + \frac{(\mathbf{c}_i \cdot \mathbf{u})^2}{2c_s^4} - \frac{\mathbf{u} \cdot u}{2c_s^2}\right). \quad (64)$$

We have the following single-step LBM algorithm:

$$\rho(\mathbf{x}, t+\delta t) = \sum_{i=1}^{N} \frac{3}{2} f^{eq}(\mathbf{x} - \mathbf{c}_i \delta t, t) - f_i^{eq}(\mathbf{x}, t) + \frac{1}{2} f_i^{eq}(\mathbf{x} + \mathbf{c}_i \delta t, t), \quad (65)$$

$$\mathbf{m}(\mathbf{x}, t+\delta t) = \sum_{i=1}^{N} c_i f_i^{eq}(\mathbf{x} - \mathbf{c}_i \delta t, t) + \quad (66)$$
$$+ \quad (\tau - 1)\mathbf{c}_i [f_i^{eq}(\mathbf{x} + \mathbf{c}_i \delta t, t) - 2 f_i^{eq}(\mathbf{x}, t) + f_i^{eq}(\mathbf{x} - \mathbf{c}_i \delta t, t)],$$

$$c(\mathbf{x}, t+\delta t) = \sum_{i=1}^{N} g_i^{eq}(\mathbf{x} - \mathbf{c}_i \delta t, t) + \quad (67)$$
$$+ \quad (\tau_c - 1)[g_i^{eq}(\mathbf{x} + \mathbf{c}_i \delta t, t) - 2 g_i^{eq}(\mathbf{x}, t) + g_i^{eq}(\mathbf{x} - \mathbf{c}_i \delta t, t)].$$

where $\mathbf{m}(\mathbf{x}, t+\delta t) = u(\mathbf{x}, t+\delta t)\rho(\mathbf{x}, t+\delta t)$.

In the GZS forcing scheme, the forcing term accounting for the external force F is written in a power series in the particle velocity

$$F_i = \left(1 - \frac{1}{2\tau}\right) w_i \left[\frac{(\mathbf{c}_i - \mathbf{u})}{c_s^2} + \frac{(\mathbf{c}_i \cdot \mathbf{u})}{c_s^4}\mathbf{c}_i\right] \cdot F_{ext} \tag{68}$$

The algorithm for the velocity field is rewritten as

$$\begin{aligned} \mathbf{u}(\mathbf{x}, t+\delta t) &= \sum_{i=1}^{N} \{\mathbf{c}_i f_i^{eq}(\mathbf{x} - \mathbf{c}_i \delta t, t) + \\ &+ (\tau - 1)\mathbf{c}_i[f_i^{eq}(\mathbf{x} + \mathbf{c}_i\delta t, t) - 2f_i^{eq}(\mathbf{x}, t) + f_i^{eq}(\mathbf{x} - \mathbf{c}_i\delta t, t)] + \\ &+ -\frac{\tau\delta t}{2}\mathbf{c}_i[F_i(\mathbf{x} + \mathbf{c}_i\delta t, t - \delta t) - F_i(\mathbf{x} - \mathbf{c}_i\delta t, t - \delta t)]\Big\} + \\ &+ F_{ext}(\mathbf{x}, t - \delta t)\delta t. \end{aligned} \tag{69}$$

With this improvement, we can simulate with multiple forms of external force interactions, including the space and time dependent body forces.

Simplified lattice Boltzmann implementation of the quasi-static approximation for pipe flows under the presence of non-uniform magnetic fields

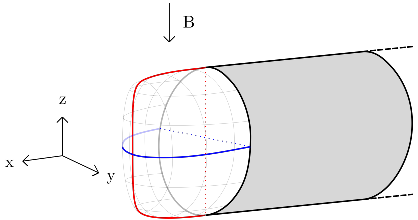

Figure: MHD pipe flow with a transversal magnetic field.

- Simulation of MDH flows using simplified LBM models;
- Improvements of recent LBM algorithms for regimes with $Re_m << 1$;
- Improved Immersed Boundary Method (IBM);
- Simulations with uniform and non-uniform magnetic fields;
- Simulations with unsteady flows.

Consider the following system:

$$\frac{\partial \mathbf{u}}{\partial t} + (\mathbf{u} \cdot \nabla)\mathbf{u} = -\frac{\nabla p}{\rho} + \nu \nabla^2 \mathbf{u} + \mathbf{J} \times \mathbf{B}, \quad (70)$$

$$\nabla \cdot \mathbf{u} = 0, \quad (71)$$

$$\partial_t \mathbf{B} + \nabla \cdot (\mathbf{u} \otimes \mathbf{B} - \mathbf{B} \otimes \mathbf{u}) = \eta \nabla^2 \mathbf{B}, \quad (72)$$

$$\nabla \cdot \mathbf{B} = 0, \quad (73)$$

where η is the (constant) **magnetic resistivity** of the fluid. The electric field $\mathbf{E}$ and the the electric current density $\mathbf{J}$ are approximated by

$$\mathbf{E} = -(\mathbf{u} \times \mathbf{B}) + \eta(\nabla \times \mathbf{B}), \qquad \mathbf{J} = \nabla \times \mathbf{B}. \quad (74)$$

Important dimensionless quantities:

$$\mathrm{Re} = \frac{UL}{\nu}, \qquad \mathrm{Re}_m = \frac{UL}{\eta}, \qquad Ha = \frac{B_0 L}{\sqrt{\eta\nu}}, \qquad Pr_m = \frac{\eta}{\nu}. \quad (75)$$

which are respectively: the **Reynolds number**, the **magnetic Reynolds number**, the **Hartmann number** and the **magnetic Prandtl number**. $\mathbf{U}$ is the characteristic velocity, $\mathbf{B}$ is the characteristic magnetic intensity and $\mathbf{L}$ is the typical length.

In the regime of $Re_m << 1$, it is convenient to introduce the decomposition $\mathbf{B} = \mathbf{B}^{ext} + \delta\mathbf{B}$, where $\mathbf{B}^{ext}$ is the external magnetic field and $\delta\mathbf{B}$ corresponds to the fluctuations. The following system holds in this situation:

$$\frac{\partial \mathbf{u}}{\partial t} + (\mathbf{u}\cdot\nabla)\mathbf{u} = -\frac{\nabla p}{\rho} + \nu\nabla^2\mathbf{u} + \mathbf{J}\times\mathbf{B}, \quad (76)$$

$$\nabla\cdot\mathbf{u} = 0, \quad (77)$$

$$\eta\nabla^2\mathbf{B} = \nabla\cdot(\mathbf{u}\otimes\mathbf{B}^{ext} - \mathbf{B}^{ext}\otimes\mathbf{u}), \quad (78)$$

$$\nabla\cdot\mathbf{B} = 0, \quad (79)$$

- The simplification eliminates the problem of a very **small magnetic diffusion time scale** in the regime $Re_m << 1$;
- But that brings up problems with the **Poisson equation**.
- Some problems with traditional **boundary conditions methods** for LBM.

Considering the following expressions for the equilibrium distributions:

$$
\begin{aligned}
f_i^{eq}(\mathbf{x},t) &= w_i\left[\rho + \left(\frac{\mathbf{c}_i\cdot\mathbf{u}}{c_s^2} + \frac{(\mathbf{c}_i\cdot\mathbf{u})^2}{2c_s^4} - \frac{\mathbf{u}\cdot\mathbf{u}}{2c_s^2}\right)\right], && (80)\\
g_{ix}^{eq}(\mathbf{x},t) &= w_i\left[B_x + \frac{c_{iy}}{c_s^2}(u_yB_x - u_xB_y) + \frac{c_{iz}}{c_s^2}(u_zB_x - u_xB_z)\right], && (81)\\
g_{iy}^{eq}(\mathbf{x},t) &= w_i\left[B_y + \frac{c_{ix}}{c_s^2}(u_xB_y - u_yB_x) + \frac{c_{iz}}{c_s^2}(u_zB_y - u_yB_z)\right], && (82)\\
g_{iz}^{eq}(\mathbf{x},t) &= w_i\left[B_z + \frac{c_{ix}}{c_s^2}(u_xB_z - u_zB_x) + \frac{c_{iy}}{c_s^2}(u_yB_z - u_zB_y)\right]. && (83)
\end{aligned}
$$

We have the following single-step LBM algorithm the for the hydrodynamic variables:

$$\rho(\mathbf{x}, t+\delta t) = \sum_{i=1}^{N} \frac{3}{2} f^{eq}(\mathbf{x}-\mathbf{c}_i\delta t, t) - f_i^{eq}(\mathbf{x}, t) + \frac{1}{2} f_i^{eq}(\mathbf{x}+\mathbf{c}_i\delta t, t), \quad (84)$$

$$\mathbf{u}(\mathbf{x}, t+\delta t) = \sum_{i=1}^{N} \mathbf{c}_i f_i^{eq}(\mathbf{x}-\mathbf{c}_i\delta t, t) + \quad (85)$$

$$+ \quad (\tau - 1)\mathbf{c}_i[f_i^{eq}(\mathbf{x}+\mathbf{c}_i\delta t, t) - 2f_i^{eq}(\mathbf{x}, t) + f_i^{eq}(\mathbf{x}-\mathbf{c}_i\delta t, t)],$$

and for the magnetic field:

$$\mathbf{B}_x(\mathbf{x}, t+\Delta t) = \sum_{i=1}^{N} g_{ix}^{eq}(\mathbf{x}-\mathbf{c}_i\delta t, t) + \quad (86)$$

$$+ \quad (\tau_m - 1)[g_{ix}^{eq}(\mathbf{x}+\mathbf{c}_i\delta t, t) - 2g_{ix}^{eq}(\mathbf{x}, t) + g_{ix}^{eq}(\mathbf{x}-\mathbf{c}_i\delta t, t)],$$

with an analogous algorithm for the other components $\mathbf{B}_y$ and $\mathbf{B}_z$.

- A fixed Eulerian mesh is applied in which the flow field is resolved, while the immersed solid boundary is described by a set if discrete Lagrangian points distributed in the fluid.

- The flow variables resolved on Eulerian mesh are corrected by a restoration force exerted from the solid boundary.

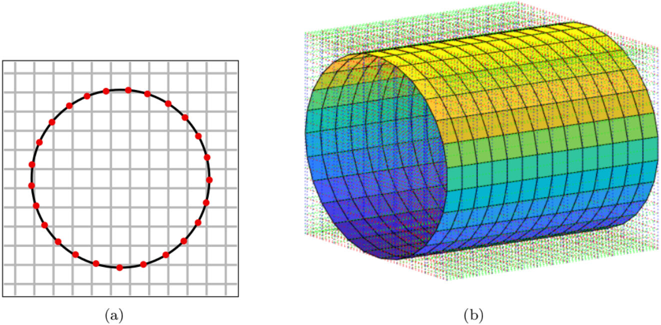

Figure: (a) Cylinder with boundary markers (in red) positioned in the fluid domain. The Eulerian and the Lagrangian meshes are independent. (b) Schematic representation of the typical immersed boundary considered for the MHD pipe flows.

The introduction of the effects of the boundaries is introduced considering a **predictor-correction algorithm**. In the predictor step, we solve the system

$$\frac{\partial \rho}{\partial t} + \nabla \cdot (\rho \mathbf{u}) = 0 \quad (87)$$

$$\frac{\partial (\rho \mathbf{u})}{\partial t} + \nabla \cdot (\rho(\mathbf{u} \otimes \mathbf{u})) = -\nabla p + \nabla \cdot \left[\mu(\nabla \mathbf{u} + \nabla \mathbf{u}^T))\right] + \mathbf{F}^{ext}. \quad (88)$$

The effects of the boundaries are imposed as an **extra forcing term introduced in the corrector step**:

$$\frac{\partial (\rho \mathbf{u})}{\partial t} = \mathbf{f}, \quad (89)$$

where $\mathbf{f}$ is determined by the IBMs to interpret boundary effects of the immersed objects.

The corrector step is discretized as

$$\rho\delta\mathbf{u} = \mathbf{f}\delta t, \tag{90}$$

where $\delta\mathbf{u}$ is the velocity correction. The velocity correction, considering the necessary scaling corrections, is given by

$$\delta\mathbf{u} = \mathbf{D}^T \begin{bmatrix} \ddots & \mathbf{0} & \mathbf{0} \\ \mathbf{0} & \frac{\lambda}{d_i(1+d_i(\lambda-1))} & \mathbf{0} \\ \mathbf{0} & \mathbf{0} & \ddots \end{bmatrix} (\mathbf{U}_b - \mathbf{D}\mathbf{u}^*). \tag{91}$$

where $\lambda = \nu_2/\nu_1$ is the viscosity ratio ($\nu_1 = 1/6$ is an optimal value for some lattice Boltzmann models), U_b is the imposed boundary condition and u^* is the velocity obtained in the predictor-step. D is an interpolating matrix whose coefficients are Lagrange polynomials and

$$d_i = \sum_{j\in\{A_{ij}\neq 0\}} A_{ij}, \quad i = 1, \cdots, N. \tag{92}$$

where

$$A_{ij} = \sum_k D(\mathbf{x}_k - \mathbf{X}_i)D(\mathbf{x}_k - \mathbf{X}_j). \tag{93}$$

where N is the number of the immersed boundary points and k are indices corresponding to the Eulerian set of points.

The flow solution can be described by a set of non-dimensional physical quantities, as the non-dimensional pressure and velocity

$$\mathbf{u}^* = \frac{\mathbf{u}}{U_r} \quad p^* = \frac{p - p_r}{\rho_r U_r^2}, \tag{94}$$

where U_r, p_r and ρ_r are reference values for velocity, pressure and density, respectively. In addition, a non-dimensional IB force is defined as

$$\mathbf{f}^* = \frac{\mathbf{f} D}{\rho_r U_r^2}. \tag{95}$$

Consider two sets of dimensional quantities $(\rho_1, \mathbf{u}_1, \mathbf{f}_1)$ and $(\rho_2, \mathbf{u}_2, \mathbf{f}_2)$, which we call systems 1 and 2 respectively. Let us also consider that the reference densities and characteristic lengths are the same, i.e., $\rho_1 = \rho_2 = \rho_r$ (small Mach numbers assumption) and $L_1 = L_2$.

The following scaling laws are verified

$$\mathbf{u}_1 = \frac{1}{\lambda}\mathbf{u}_2, \quad \mathbf{f}_1 = \frac{1}{\lambda^2}\mathbf{f}_2, \tag{96}$$

where $\lambda = \nu_2/\nu_1$ with ν_1 and ν_2 being the viscosities. The IB forces can be rewritten as

$$\mathbf{f}_1 = \rho_r \delta \mathbf{u}_2 = \rho_r(\mathbf{u}_1 - \mathbf{u}_1^*), \qquad \mathbf{f}_2 = \rho_r \delta \mathbf{u}_2 = \rho_r(\mathbf{u}_2 - \mathbf{u}_2^*), \tag{97}$$

which leads to the the following equation

$$\mathbf{u}_1^* = \left(\frac{1}{\lambda} - \frac{1}{\lambda^2}\right)\mathbf{u}_2 + \frac{1}{\lambda^2}\mathbf{u}_2^*. \tag{98}$$

This property leads to a numerical error in many explicit immersed boundary methods.

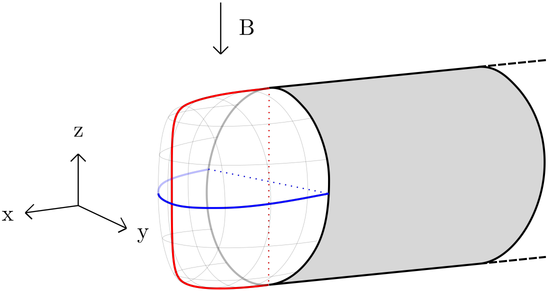

Figure: Schematic representation of MHD pipe flow with a transversal magnetic field.

The velocity and magnetic field distributions are given by the analytical solution developed by Richard R. Gold[4].

[1]Gold, Richard R. "Magnetohydrodynamic pipe flow. Part 1." Journal of Fluid Mechanics 13.4 (1962): 505-512.

The Gold's solutions for the streamwise components of velocity and magnetic fields are given by

$$U_x(r,\theta) = -\frac{R^2}{\nu Ha}\frac{\partial p}{\partial x}\left[\cosh(\alpha r\cos\theta)\sum_{n=0}^{\infty}\varepsilon_n\frac{I'_{2n}(\alpha)}{I_{2n}(\alpha)}I_{2n}(\alpha r)\cos(2n\theta) - \right.$$
$$\left. - \sinh(\alpha r\cos\theta)\sum_{n=0}^{\infty}2\frac{I'_{2n+1}(\alpha)}{I_{2n+1}(\alpha)}I_{2n+1}(\alpha r)\cos((2n+1)\theta)\right],$$
$$B_x(r,\theta) = -\frac{1}{\sqrt{\eta\nu}}\frac{R^2}{2Ha}\frac{\partial p}{\partial x}\left[\sum_{n=-\infty}^{\infty}(\exp(-\alpha r\cos\theta) - \right.$$
$$\left. - (-1)^n\exp(\alpha r\cos\theta))\frac{I'_n(\alpha)}{I_n(\alpha)}I_n(\alpha r)\exp(in\theta) - 2r\cos\theta\right],$$

where $\alpha = Ha/2$, ϵ_n equal 1 for $n=0$ and 2 for $n>0$. I_n is the modified Bessel function of the first kind of order n and I'_n is the respective derivative.

Viscosity-independent boundary condition-enforced IBM

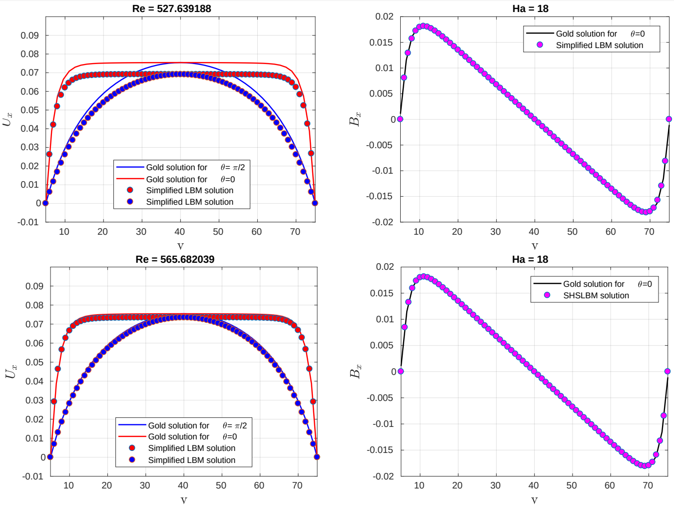

Figure: Simulation of MHD pipe flows under the presence of a transversal magnetic field with viscosity $\nu = 0.004$, resistivity $\eta = 0.04$ and $Ha = 18$. In these experiments, we show the magnetic and velocity field profiles for a simulation with pipe radius $r = 35$ and constant pressure difference $\frac{\partial p}{\partial x} = -3.7 \times 10^{-5}$, and we compare with the respective analytical solutions.

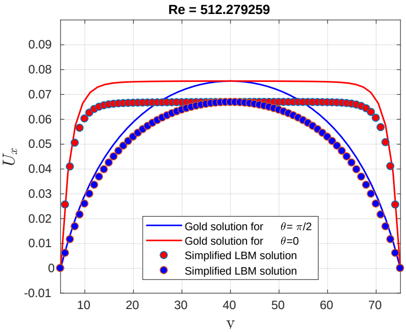

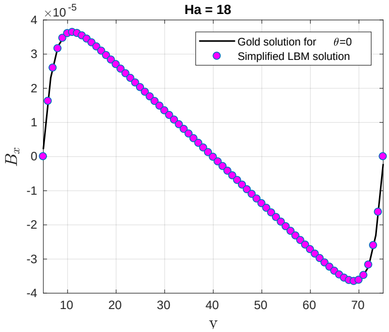

Figure: Comparison with the Gold's solutions by using the single-step LBM algorithms with viscosity $\nu = 0.004$, resistivity $\eta = 10000$ and Hartman number $Ha = 18$ in a pipe with radius $r = 35$. The algorithm for the magnetic field is iterated $N_{mag} = 12$ times before every update of the velocity field. The resulting magnetic Prandtl number $Pr_m = 4 \times 10^{-7}$.

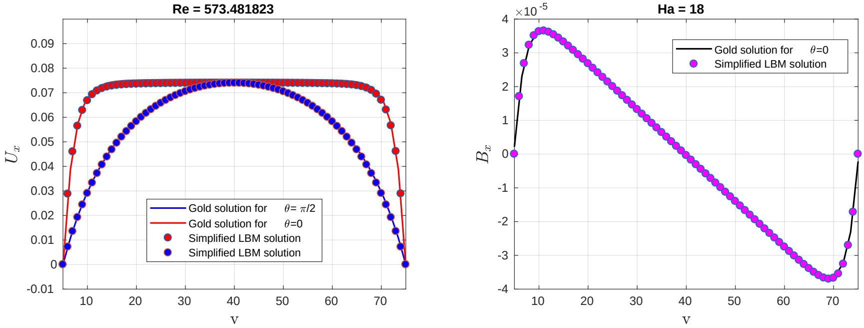

Figure: Comparison with the Gold's solutions by using the single-step LBM algorithms with viscosity $\nu = 0.004$, resistivity $\eta = 10000$ and Hartman number $Ha = 18$ in a pipe with radius $r = 35$. The algorithm for the magnetic field is iterated $N_{mag} = 12$ times before every update of the velocity field. The resulting magnetic Prandtl number $Pr_m = 4 \times 10^{-7}$.

We analyse the evolution of magnetic energy $E_m = \left\langle \frac{1}{2}|B|^2 \right\rangle$ and the kinetic energy $E_k = \left\langle \frac{1}{2}\rho|\mathbf{u}|^2 \right\rangle$ (per unit of volume) where $\langle \cdot \rangle$ denotes spatial averages within a cylinder with radius smaller than the radius of the pipe. Their variations are obtained given by

$$\begin{aligned} \frac{dE_m}{dt} &= \eta \left\langle \mathbf{B} \cdot \nabla^2 \mathbf{B} \right\rangle - \langle \mathbf{B} \cdot (\nabla \cdot (\mathbf{uB} - \mathbf{Bu})) \rangle , \quad (99) \\ \frac{dE_k}{dt} &= -\langle \mathbf{u} \cdot \nabla p \rangle + \left\langle \mathbf{u} \cdot \left[\nabla \cdot \left(\mu \nabla \mathbf{u} + \mu \nabla \mathbf{u}^T \right) \right] \right\rangle + \langle \mathbf{u} \cdot (\mathbf{J} \times \mathbf{B}) \rangle . \end{aligned}$$

We also analyse the situation with unsteady flow by introducing a variable pressure difference as follows

$$\frac{\partial p}{\partial x} = -F_0 \cos\left(\frac{2\pi t}{T}\right), \quad (100)$$

where F_0 is a value of reference and T is the period. In our applications we choose $T = 200$.

Energy budget analysis and unsteady flows

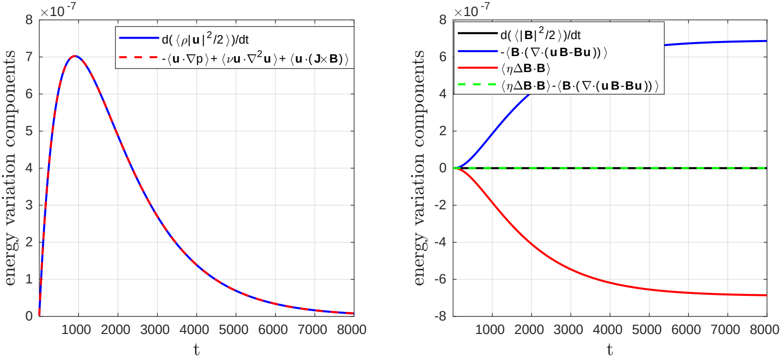

Figure: Verification of the Gold solution by using the single-step LBM with viscosity $\nu = 0.04$, resistivity $\eta = 10000$ and Hartman number $Ha = 18$. The simulation is starts from the zero velocity configuration and evolves until it reaches the stationary regime.

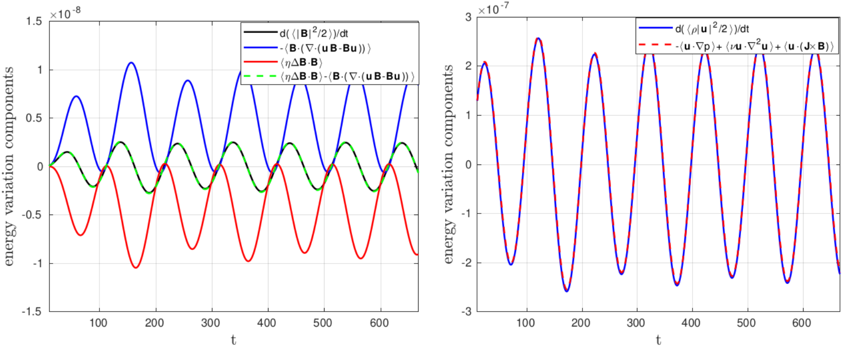

Figure: Simulation of the MHD flow in a circular pipe with radius $r = 22$, $Ha = 18$, $\eta = 2$ and $\nu = 0.08$ submitted to $\partial p/\partial x = -0.00024\cos(2\pi t/200)$. The algorithm for the magnetic field performs $1/dt = N = 12$ iterations before every time step of the algorithm for the velocity field.

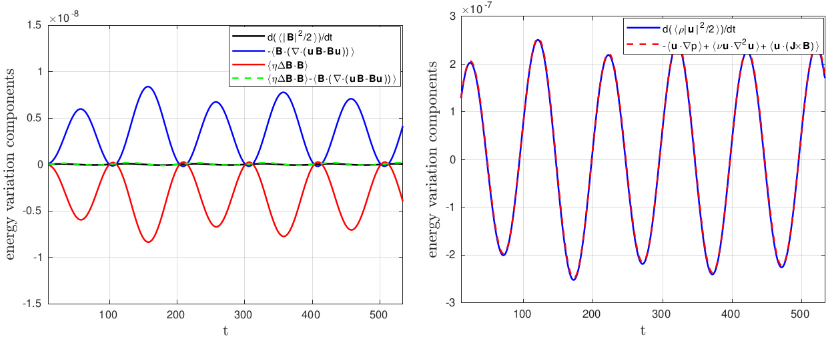

Figure: Simulation of the MHD flow in a circular pipe with radius $r = 22$, $Ha = 18$, $\eta = 45$ and $\nu = 0.08$ submitted to $\partial p/\partial x = -0.00024\cos(2\pi t/200)$. The algorithm for the magnetic field performs $1/dt = N = 270$ iterations before every time step of the algorithm for the velocity field.

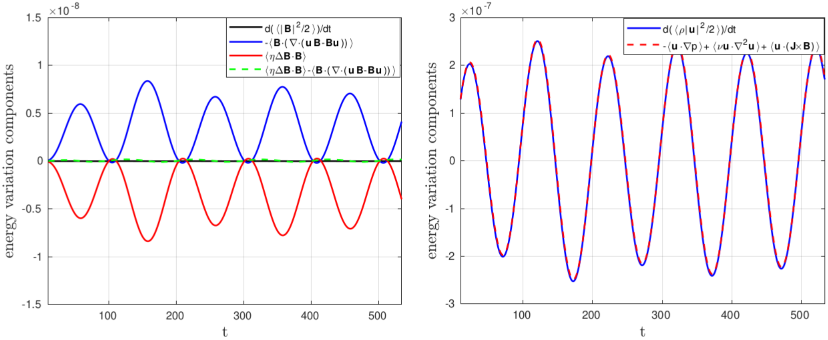

Figure: Simulation of the MHD flow in a circular pipe with radius $r = 22$, $Ha = 18$, $\eta = 1000$ and $\nu = 0.08$ submitted to $\partial p/\partial x = -0.00024\cos(2\pi t/200)$. The algorithm for the magnetic field performs $1/dt = N = 270$ iterations before every time step of the algorithm for the velocity field.

Non-uniform magnetic fields

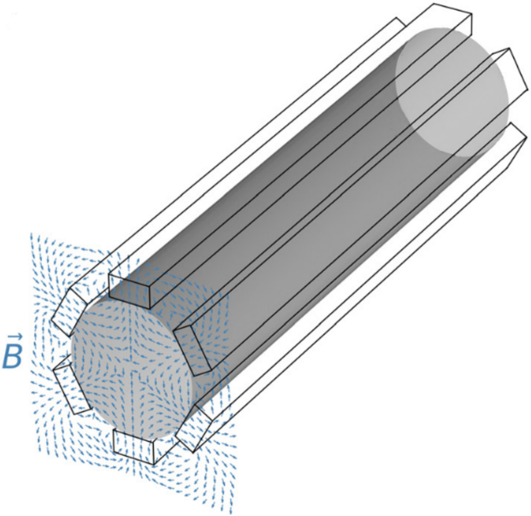

Figure: Schematics of the pipe flow setup with a representation of the positions of the six covering magnetic slabs.

Non-uniform magnetic fields

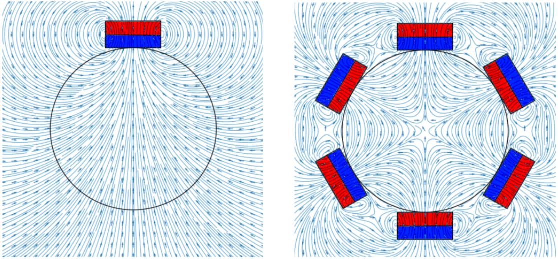

(a) (b)

Figure: (a) Magnetic field lines of one magnet generated by the field given by (107) and (108) in the yz-plane, where the red and blue colors indicate the north and south poles of the magnets, respectively. In (b), the magnetic field lines generated by a set of six magnets with alternating poles forming an hexagonal structure

The analytical expression for the magnetic field of one magnet is given by:

$$\mathbf{B}_x(x,y) = 2\left[tan^{-1}\left(\frac{x-L}{y}\right) - tan^{-1}\left(\frac{x+L}{y}\right)\right], \quad (101)$$

$$\mathbf{B}_y(x,y) = \log\left(\frac{(x+L)^2+y^2}{(x-L)^2+y^2}\right). \quad (102)$$

Non-uniform magnetic fields

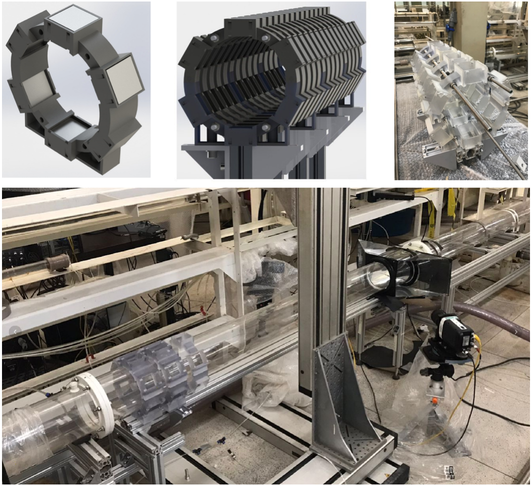

Figure: Project PRIMATE (Pipe Rig for the Investigation of Magnetic Fields). Project in collaboration with Luca Moriconi, Bruno Magacho and Juliana B.R. Loureiro from UFRJ.

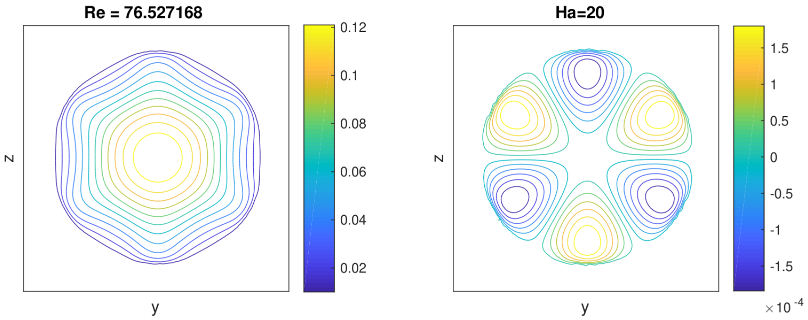

(a) (b)

Figure: Simulation of a MHD flows with the six magnets configuration in the quasi-static regime with $\eta = 1000$, $Ha = 20$, $\nu = 0.04$ and pipe radius $r = 38.5$. A constant body force with $\frac{\partial p}{\partial x} = -2.16 \times 10^{-5}$ is applied. The simulation is performed until the stationary solution is obtained. In (a) and (b) we show some level curves for the velocity and magnetic fields, respectively.

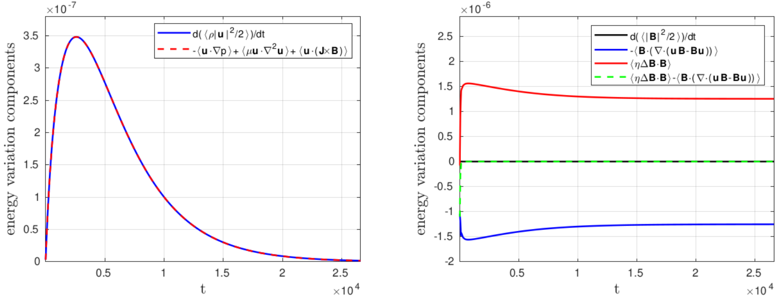

Figure: Simulation of a MHD flows with the six magnets configuration in the quasi-static regime with $\eta = 1000$, $Ha = 20$, $\nu = 0.04$ and pipe radius $r = 38.5$. A constant body force with $\frac{\partial p}{\partial x} = -2.16 \times 10^{-5}$ is applied. The simulation is performed until the stationary solution is obtained. In (c) we show the verification of the energy balance equations.

The space-time evolution for the Central-Moments LBM are obtained according to

$$f_i(\mathbf{x} + c_i, t+1) - f_i(\mathbf{x}, t) = -\mathbf{\Omega}_{CM} f_i^{neq}(\mathbf{x}, t) \tag{103}$$

where f_i^* are the post-collision VDFs. The CM-LBM can be summarized by

$$\mathbf{\Omega}_{CM} = \mathbf{M}^{-1}\mathbf{N}^{-1}\mathbf{SNM}, \qquad f^{neq} = (f_i - f_i^{eq,ext}) \tag{104}$$

where $\mathbf{N}$ and $\mathbf{N}^{-1}$ are the velocity dependent matrices used to move **from the raw to the central moment space**, and vice-versa. $\mathbf{M}$ and $\mathbf{M}^{-1}$ are commonly defined as orthogonal matrices allowing us to move **from the velocity space to the to the raw moment space**, and f_i^{eq} is the extended equilibrium state that includes up to sixth order terms. **S** is the **collision matrix**.
For the magnetic field LBM, it follows the MRT according to

$$g_{i,\alpha}(\mathbf{x} + c_i, t+1) - g_{i,\alpha}(\mathbf{x}, t) = -\mathbf{M}^{-1}\mathbf{SM}g_{i,\alpha}^{neq}(\mathbf{x}, t) \tag{105}$$

For the velocity field distributions it is applied the Bouzidi's technique, for the vector valued distributions its proposed an extension from a LBM for advection-diffusion boundary condition

$$\mathbf{g}_{\bar{i},\alpha}(\mathbf{x}_f, t+1) = 2(\Delta - 1)\tilde{\mathbf{g}}_{i,\alpha}(\mathbf{x}_f, t) - \left(\frac{(2\Delta-1)^2}{2\Delta+1}\right)\tilde{\mathbf{g}}_{i,\alpha}(\mathbf{x}_{ff}, t) + 2\left(\frac{2\Delta-1}{2\Delta+1}\right)\tilde{\mathbf{g}}_{\bar{i},\alpha}(\mathbf{x}_f, t) + \frac{1}{3}\left(\frac{3-2\Delta}{2\Delta+1}\right)B_\alpha|_{wall} \quad (106)$$

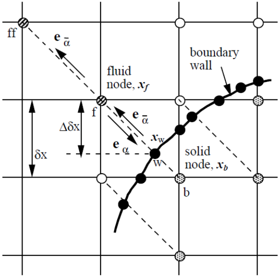

Figure: Layout of the regularly spaced lattices and curved wall boundary. Source: Yu et all (2003).

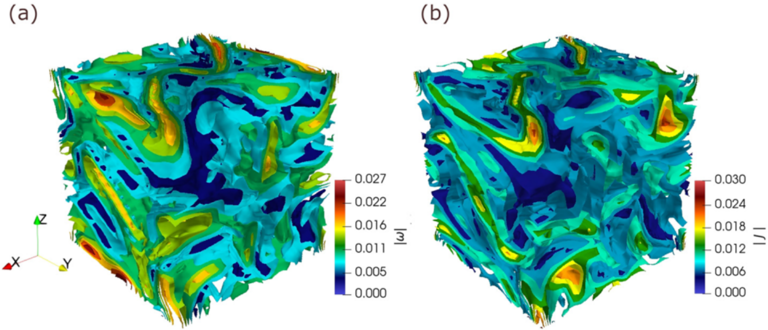

Figure: Absolute values of (a) vorticity and (b) current density. Both cases have $Re = 2000$ and $R_m = 200$.

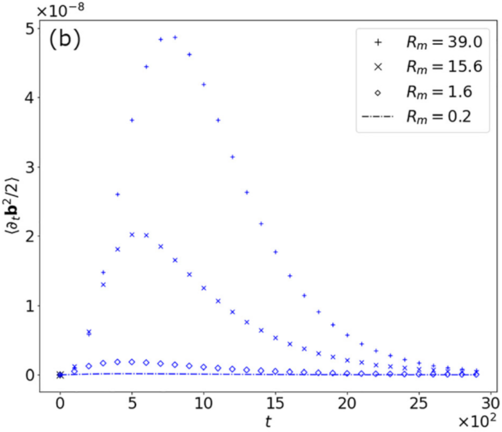

Figure: A closer look at the time evolution of the magnetic energy for various R_m .

Final remarks

- We provide a **set of extensions and improvements** in a class of simplified LBM algorithms with the objective of simulating MHD flows with **very small magnetic Reynolds numbers** in pipe flows;
- We also introduce an **immersed boundary method** which is able to accurately include the effects curved insulating walls in the MHD equations and whose **accuracy is not significantly dependent on the values of the relaxation times**;
- Improvements in the implementation of forcing term allows an **accurate and stable inclusion of variable forcing terms**, showing good results even in the presence of strongly non-uniform magnetic fields;
- We provide a **completely local and explicit LBM framework** for simulations of the quasi-static approximation in pipe flows, with a good potential for simulations involving more complex geometries.

- Tavares, H. S., Magacho, B., Moriconi, L., Loureiro, J. B. (2023).*A simplified lattice Boltzmann implementation of the quasi-static approximation in pipe flows under the presence of non-uniform magnetic fields*. Computers Mathematics with Applications, 148, 93-112.
- Magacho, B., Tavares, H. S., Moriconi, L., Loureiro, J. B. R. (2023). *Double multiple-relaxation-time model of lattice-Boltzmann magnetohydrodynamics at low magnetic Reynolds numbers. Physics of Fluids, 35(1).*
- Krüger, T., Kusumaatmaja, H., Kuzmin, A., Shardt, O., Silva, G., Viggen, E. M. (2017). *The lattice Boltzmann method*. Springer International Publishing, 10(978-3), 4-15.
- Dellar, P. J. (2002). *Lattice kinetic schemes for magnetohydrodynamics*. Journal of Computational Physics, 179(1), 95-126.

De Rosis, A., Liu, R., Revell, A. (2021). *One-stage simplified lattice Boltzmann method for two-and three-dimensional magnetohydrodynamic flows*. Physics of Fluids, 33(8).

Delgado-Gutiérrez, A., Marzocca, P., Cardenas, D., Probst, O. (2021).*A single-step and simplified graphics processing unit lattice Boltzmann method for high turbulent flows*. International Journal for Numerical Methods in Fluids, 93(7), 2339-2361.